

## CHAPTER 135

### THREE DESIGN SYSTEMS FOR APPLICATIONS IN COASTAL ENGINEERING

M.B. Abbott,  
International Courses, Oude Delft 95, Delft, Netherlands;  
Computational Hydraulics Centre, Danish Hydraulic Institute, Øster  
Voldgade 10, 1350 Copenhagen K, Denmark;

J. Aa. Bertelsen, Aa. Damsgaard, P.I. Hinstrup, G.S. Rodenhuis and  
R.I. Warren,  
Computational Hydraulics Centre, Danish Hydraulic Institute, Øster  
Voldgade 10, 1350 Copenhagen K, Denmark;

and A. Verwey,  
International Courses, Oude Delft 95, Delft, Netherlands.

#### 1. INTRODUCTION

The Computational Hydraulics Centre in Copenhagen has developed three design systems for applications in hydraulics, coastal and offshore engineering. Each system constitutes a software - documentation entity that automatically constructs and runs mathematical models of a specific class when presented only with the model description. The systems concerned are as follows:

System 11, "Siva", is restricted to 1-dimensional flows of 1-layer (vertically homogeneous) fluids.

System 21, "Jupiter", applies to 2-dimensional flows of 1-layer fluids.

Systems 12/13 and 22/23, "Neptune", apply to 1-dimensional flows with 2 or 3 layers for the 12/13 and 2-dimensional flows with 2 or 3 layers for the 22/23.

Brief descriptions of these systems follow.

#### 2. SYSTEM 11, "SIVA"

This system can be used to describe unsteady nearly-horizontal flows in any system of channels, taking account of changes in flow section with elevation and related effects on mean flow paths, resistances, dispersion etc. The system is built upon the equations of conservation of mass and momentum, together with transport - dispersion - dilution - reaction equations for salt, BOD and oxygen, as follows:

$$\frac{\partial}{\partial t} \left( \frac{\partial h}{\partial t} + \frac{\partial Q}{\partial x} \right) = q \quad (1)$$

$$\begin{aligned} \frac{\partial Q}{\partial t} + \frac{\partial}{\partial x} \left( \frac{\alpha \rho Q^2}{A} \right) + \frac{\rho g A \partial h}{\partial x} + \frac{\rho g Q |Q|}{C^2 A R} - \rho_q q |v| \cos \theta \\ + \frac{Q \partial C}{\partial t} + f(h) \frac{\partial C}{\partial x} = 0 \end{aligned} \quad (2)$$

$$A_v \frac{\partial C}{\partial t} + \frac{Q \partial C}{\partial x} - \frac{\partial}{\partial x} \left( AD \frac{\partial C}{\partial x} \right) = q(c_q - c) \quad (3)$$

$$A_v \frac{\partial L}{\partial t} + \frac{Q \partial L}{\partial x} - \frac{\partial}{\partial x} \left( AD \frac{\partial L}{\partial x} \right) + (K_1 - K_3) A_v L = q(L_q - L) \quad (4)$$

$$A_v \frac{\partial I}{\partial t} + \frac{Q \partial I}{\partial x} - \frac{\partial}{\partial x} \left( AD \frac{\partial I}{\partial x} \right) + K_1 A_v L - K_2 A_v (I_q - I) = q(I_q - I) \quad (5)$$

Equations similar to (3, 4, 5) can be introduced to describe pollution due to heat and various chemicals. Fig. 1-2 shows some properties of the model constructed for field testing the system on the Limfjord, in Northern Denmark.

### 3. SYSTEM 21, "JUPITER"

The "Jupiter" is applied to investigations in seas, more complicated estuaries, harbour, lakes and similar bodies of water. The equations of mass and momentum solved by the system read as follows:

$$\frac{\partial (\rho h)}{\partial t} + \frac{\partial (\rho p)}{\partial x} + \frac{\partial (\rho q)}{\partial y} = 0 \quad (6)$$

$$\begin{aligned} \frac{\partial (\rho p)}{\partial t} + \frac{\partial}{\partial x} \left( \frac{(\rho p)^2}{h} \right) + \frac{\partial}{\partial y} \left( \frac{\rho p q}{h} \right) + g h \frac{\partial}{\partial x} (\rho(h-H)) \\ - \Omega \rho q + \frac{\rho g}{C^2 h} \sqrt{p^2 + q^2} \cdot p - w_x \rho = 0 \end{aligned} \quad (7)$$

$$\begin{aligned} \frac{\partial (\rho q)}{\partial t} + \frac{\partial}{\partial y} \left( \frac{\rho q^2}{h} \right) + \frac{\partial}{\partial x} \left( \frac{\rho p q}{h} \right) + g h \frac{\partial}{\partial y} (\rho(h+H)) \\ + \Omega \rho p + \frac{\rho g}{C^2 h} \sqrt{p^2 + q^2} \cdot q - w_y \rho = 0 \end{aligned} \quad (8)$$

Further, equations generalised from (3, 4, 5) can be superimposed, to constitute a "pollution superstructure".

The Jupiter has been extensively developed in several versions, referred to as "Marks". In the Mark 1, special forms of equations (6, 7, 8) are used along grid lines running adjacent to coasts, so that the model topography is resolved to a high level of accuracy - comparable with the "free grid" of the finite-element method. In the Mark 2 further facilities are introduced to allow flooding and drying within the model. The Mark 3 allows, in addition, several changes of scale within a single model, with step-down ratios in grid size of 2 or 3 at each change. The version carrying the pollution superstructure is called the Mark 4. Finally there is a Mark 5 that suppresses the special forms of (6, 7, 8) along beaches, so as to work in "minimum configuration". The identifiers can be combined, to give, for example, a Mark 52 or a Mark 53.

The Marks 1, 2 and 52 have been used extensively over the last three years while the Mark 53 has been field tested. Some results are shown in Fig. 3-5.

#### 4. SYSTEMS 12/13 AND 22/23, "NEPTUNE"

The hydrodynamic "platform" program of the 12/13 is built upon equations of conservation of mass, linear momentum and density deficit. For the System 12 these equations read as follows:

$$\frac{\partial}{\partial t}(\rho_1 h_1) + \frac{\partial}{\partial x}(\rho_1 u_1 h_1 + (\rho_0 q_0 - \rho_1 q_1)) = 0 \quad (9)$$

$$\frac{\partial}{\partial t}(\rho_0 h_0) + \frac{\partial}{\partial x}(\rho_0 u_0 h_0) + (\rho_1 q_1 - \rho_0 q_0) = 0 \quad (10)$$

$$\begin{aligned} \frac{\partial}{\partial t}(\rho_1 u_1 h_1) + \frac{\partial}{\partial x}(\rho_1 u_1^2 h_1) + \rho_1 g h_1 \frac{\partial}{\partial x}(H + h_1 + h_0) \\ + (\rho_0 q_0 u_0 - \rho_1 q_1 u_1) = 0 \end{aligned} \quad (11)$$

$$\begin{aligned} \frac{\partial}{\partial t}(\rho_0 u_0 h_0) + \frac{\partial}{\partial x}(\rho_0 u_0^2 h_0) + \rho_0 g h^0 \frac{\partial}{\partial x}(H + \rho_1 h_1 + h_0) \\ - (\rho_1 q_1 u_1 - \rho_0 q_0 u_0) = 0 \end{aligned} \quad (12)$$

$$\frac{\partial \rho_1}{\partial t} + u_1 \frac{\partial \rho_1}{\partial x} - \frac{\rho_1}{\rho_w} \frac{\partial^2 \rho_1}{\partial x^2} + \frac{q_0}{h_0} (\rho_0 - \rho_1) = 0 \quad (13)$$

$$\frac{\partial \rho_0}{\partial t} + \frac{u_0 \partial \rho_0}{\partial x} - \frac{\rho_0}{\rho_w} \frac{\partial^2 \rho_0}{\partial x^2} - \frac{q_1(\rho_i - \rho_0)}{h_0} = 0 \quad (14)$$

In addition, a bed stress, a surface (wind) stress and an interfacial stress may be introduced. The equations generalise easily to three layers and also to two dimensions. The systems can be used for three-dimensional modelling, when  $h_0$ ,  $h_1$  and  $h_2$ , for three layers, correspond to vertical Lagrangian coordinates, but the rate of vertical mixing in the physical and numerical stabilising processes remains unclear.

In both 12/13 and 22/23, pollution "superstructures" can be mounted, to describe the transport, dispersion, reaction etc. of various substances. Fig. 6 shows some results from field tests of the System 12 on the Gota river in South Sweden

### 5. CONCLUSIONS

The System 21, "Jupiter" is now a well tried instrument in coastal engineering, providing considerable economics in field investigations. The System 11, "Siva", and the 12/13 part of the "Neptune" are currently becoming operational on a commercial basis while the 22/23 is the subject of intensive development and should be available commercially during 1975.

### 6. NOTATION

$b_s$	(m)	storage width
$c$		salt concentration
$f(h)$	( $m^4/s^2$ )	function of the depth squared integrated over the crosssection
$g$	( $m/s^2$ )	acceleration due to gravity
$h$	(m)	level above arbitrary horizontal reference level
$k_1$	( $s^{-1}$ )	coefficient of BOD decay due to oxidation
$k_2$	( $s^{-1}$ )	coefficient of reaeration
$k_3$	( $s^{-1}$ )	cooefficient of BOD decay due to other processes
$q$	( $m^2/s$ )	lateral inflow
$t$	(s)	time
$u$	( $m/s$ )	velocity in x-direction
$v$	( $m/s$ )	lateral inflow velocity, velocity in y-direction
$x$	(m)	coordinate along the river, West-East coordinate
$Y$	(m)	South-North coordinate
$A$	( $m^2$ )	flow area perpendicular to the stream

$A_v$	( $m^2$ )	storage area perpendicular to the stream (integral of $b_s$ over depth)
$C$	( $m^{\frac{1}{2}}/s$ )	Chezy resistance value
$D$	( $m^2/s$ )	coefficient of longitudinal dispersion
$H$	(m)	elevation of bed, above datum
$I$		dissolved oxygen concentration
$I_s$		saturation concentration of dissolved oxygen
$L$		BOD concentration
$Q$	( $m^3/s$ )	volume flux of fluid
$R$	(m)	hydraulic radius
$\alpha$		crosssectional velocity distribution coefficient.
$\rho$	( $kg/m^3$ )	fluid density

System 11 figures.

Hydrodynamic Model of the Limfjord, North Jutland.

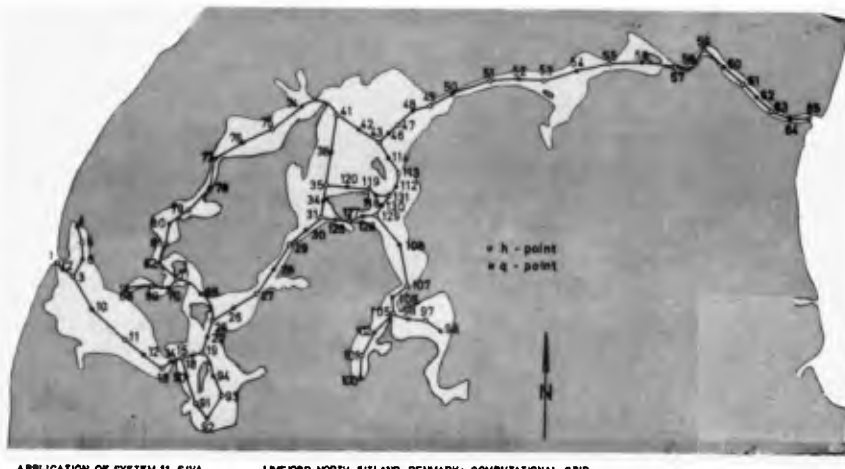


Fig. 1A

Computational Grid

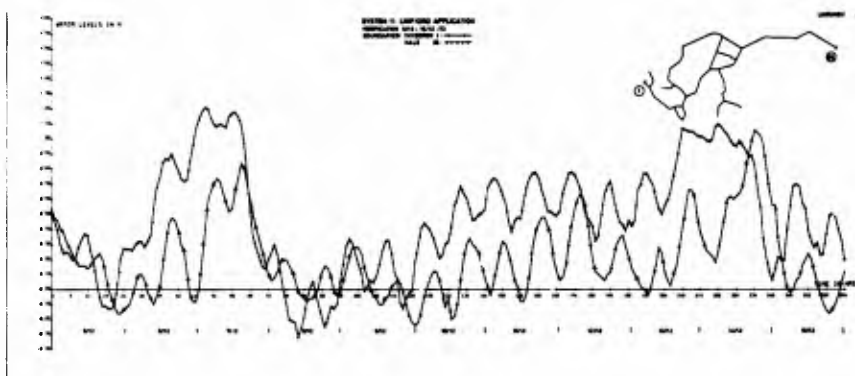


Fig. 1B

Water levels at Boundaries

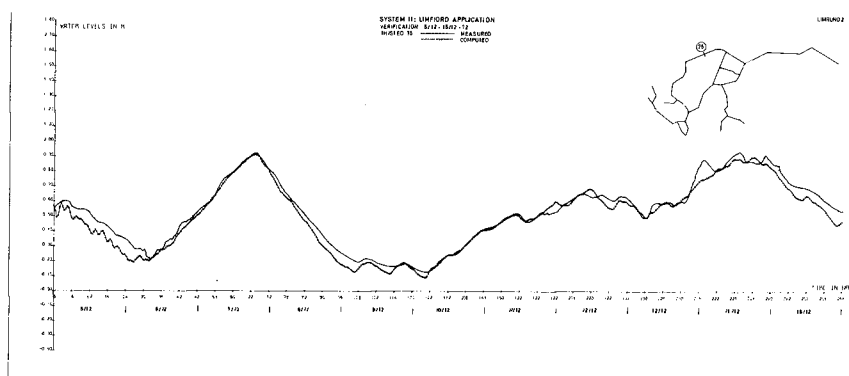


Fig. 1C Computed and Recorded Water Levels

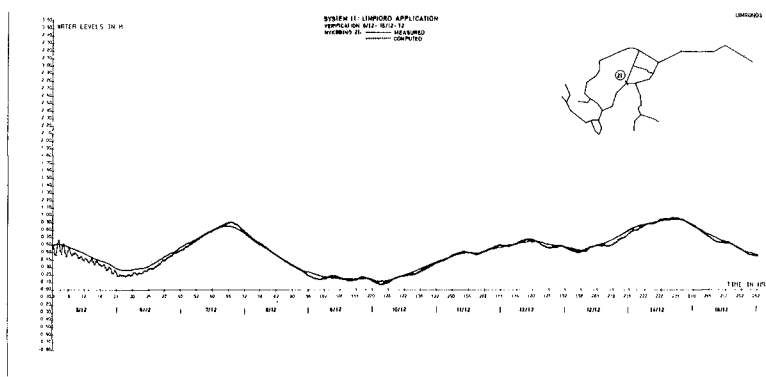


Fig. 1D  
Computed and Recorded Water Levels

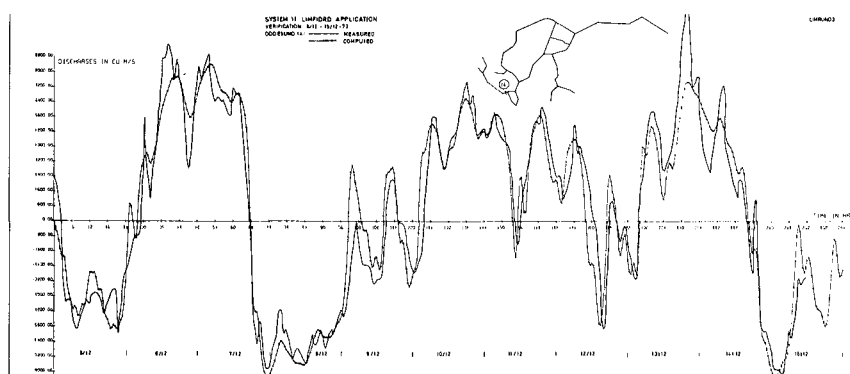


Fig. 1E      Computed and Recorded Discharges

## Transport-Dispersion Model

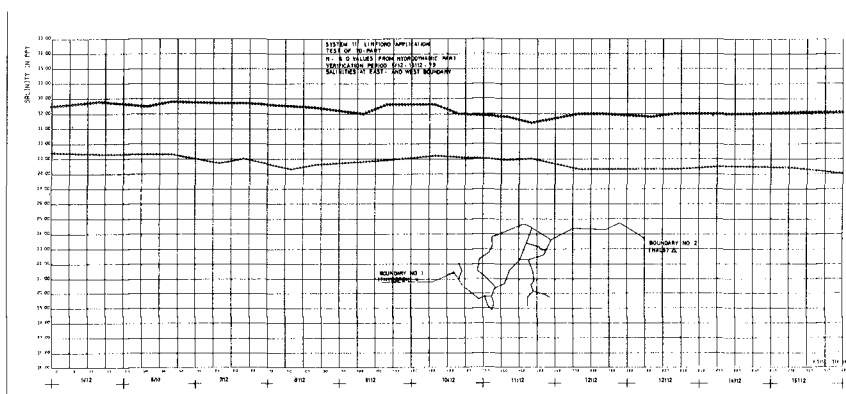


Fig. 2A

Recorded Salinities at Boundaries

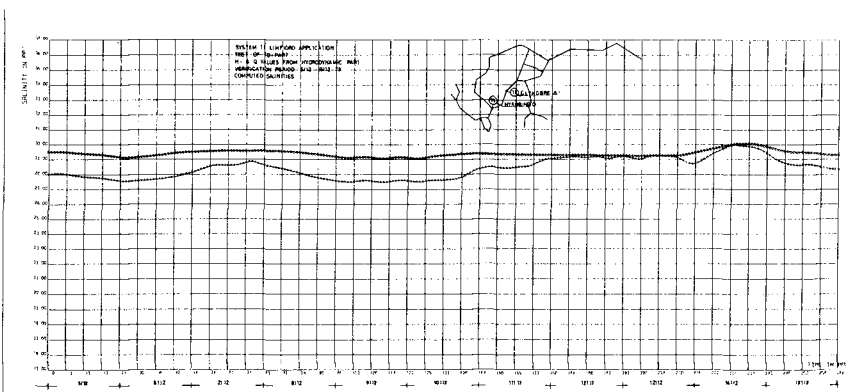


Fig. 2B

Computed Salinities

System 21 figures.

Model of Hurricane Surges in Key Biscayne, Florida

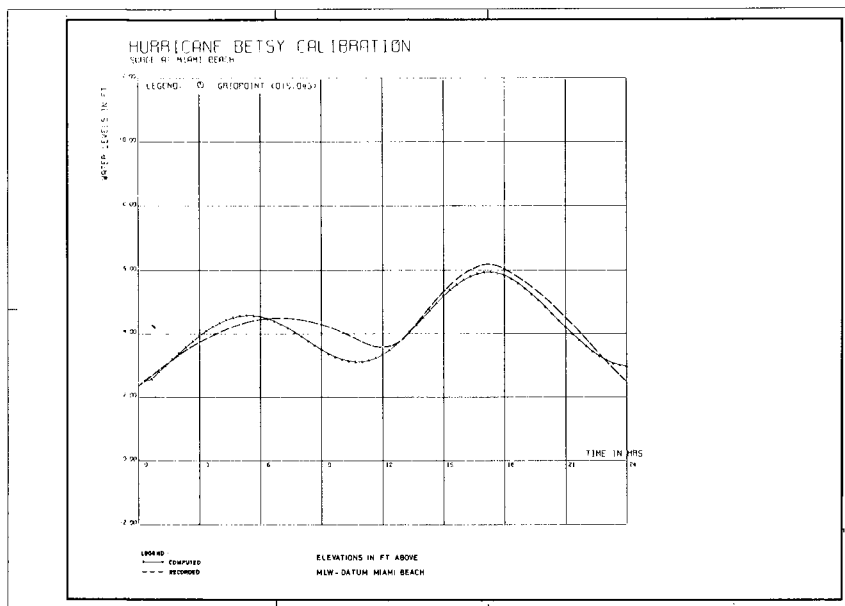


Fig. 3a

Calibration of the model using Hurricane "Betsy" data.

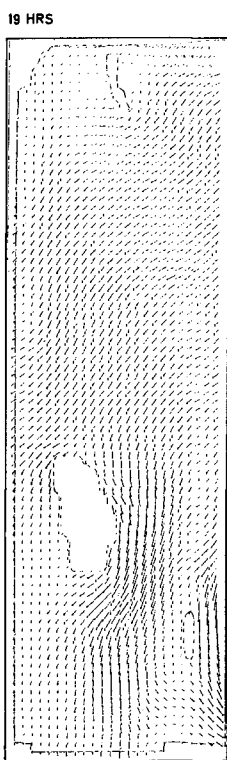


Fig. 3b  
Plot of fluxes ( $\text{ft}^2 \cdot \text{s}^{-1}$ )  
19 hrs. after start of  
test.

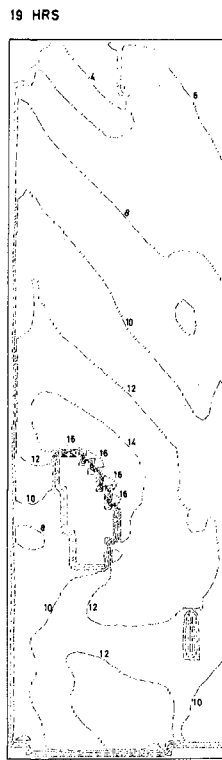


Fig. 3c  
Plot of water level contours (ft)  
19 hrs. after start of test.

## Model of an Instantaneous Dam Failure.

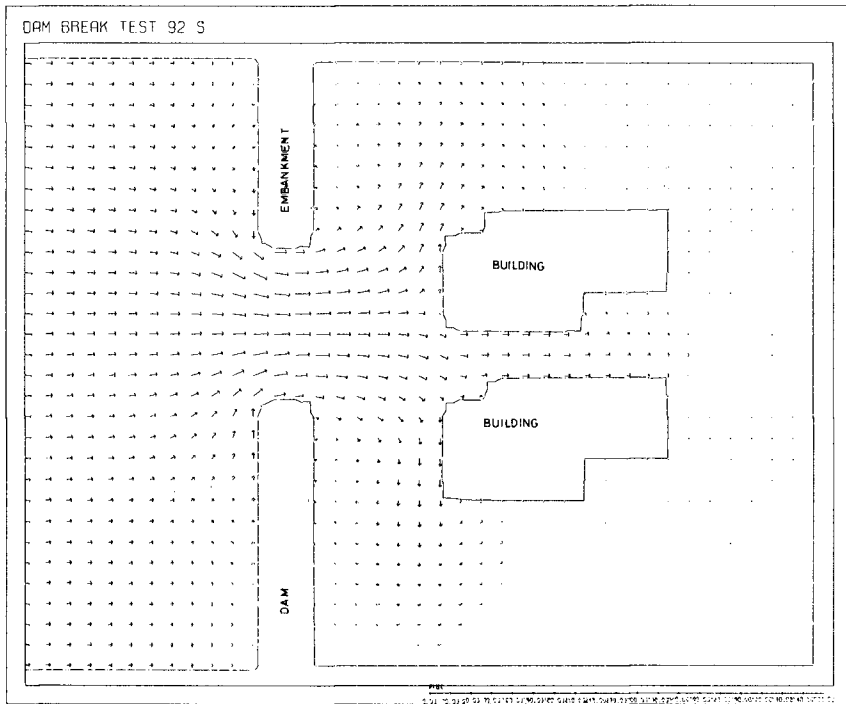


Fig. 4a  
 Plot of fluxes ( $m^2 \cdot s^{-1}$ )  
 92 sec. after failure.

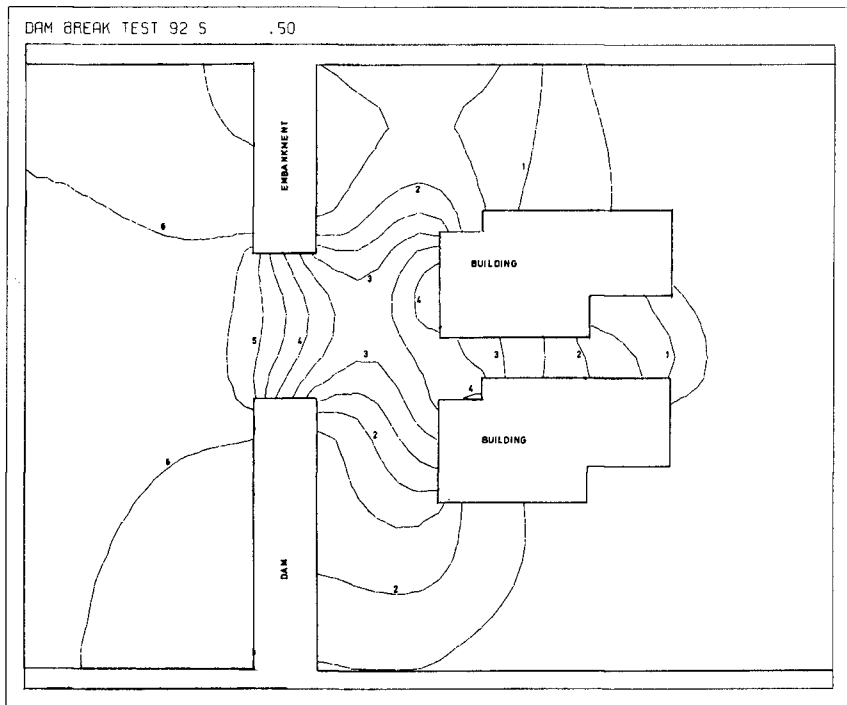


Fig. 4b  
Plot of water level contours (m)  
92 sec. after failure.

Model of Harbour Seiches.

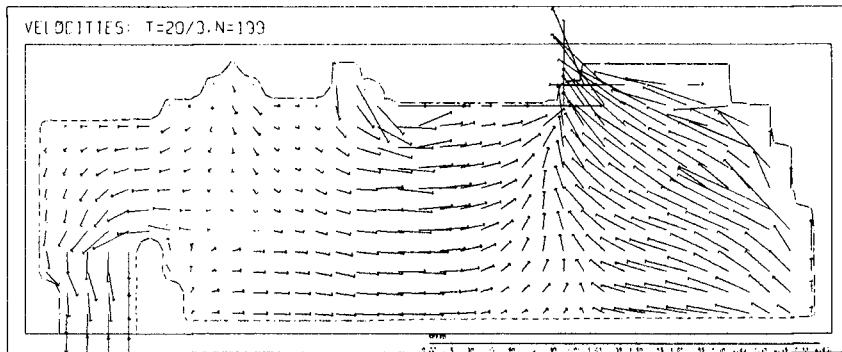


Fig. 5A

Plot of fluxes ( $\text{m}^2 \cdot \text{s}^{-1}$ ) at an instant during a full wave mode of oscillation.

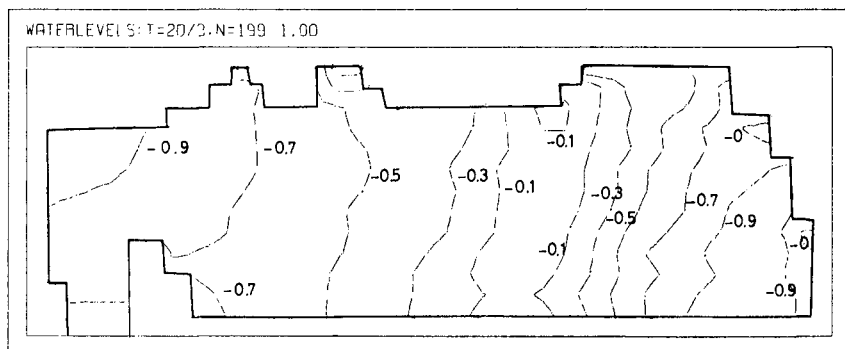


Fig. 5B

Plot of water level contours (m) at an instant during a full wave mode of oscillation.

System 12 figures.

## Model of the Göta River, Sweden

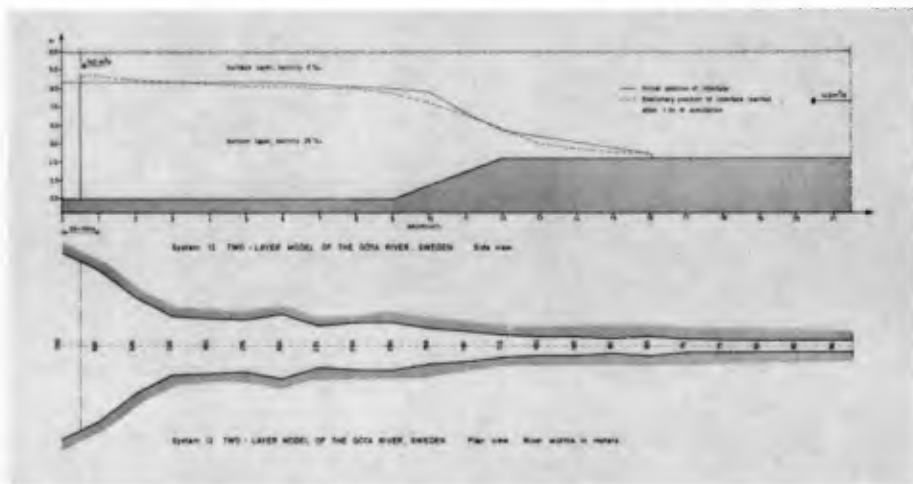


Fig. 6

Computed Positions of Interface